

Measurement of the hyperfine structure of the $S_{1/2} - D_{5/2}$ transition in $^{43}\text{Ca}^+$

J. Benhelm^{1,*}, G. Kirchmair¹, U. Rapol^{1,†}, T. Körber¹, C. F. Roos^{1,2}, and R. Blatt^{1,2‡}

¹*Institut für Experimentalphysik, Universität Innsbruck, Technikerstr. 25, A-6020 Innsbruck, Austria*

²*Institut für Quantenoptik und Quanteninformation,*

Österreichische Akademie der Wissenschaften, Otto-Hittmair-Platz 1, A-6020 Innsbruck, Austria

(Dated: April 29, 2019)

The hyperfine structure of the $4s^2S_{1/2} - 3d^2D_{5/2}$ quadrupole transition at 729 nm in $^{43}\text{Ca}^+$ has been investigated by laser spectroscopy using a single trapped $^{43}\text{Ca}^+$ ion. We determine the hyperfine structure constants of the metastable level as $A_{D_{5/2}} = 3.8931(2)$ MHz and $B_{D_{5/2}} = 4.241(4)$ MHz. The isotope shift of the transition with respect to $^{40}\text{Ca}^+$ was measured to be $\Delta_{iso}^{43,40} = 4134.713(5)$ MHz. We demonstrate the existence of transitions that become independent of the first-order Zeeman shift at non-zero low magnetic fields. These transitions might be better suited for building a frequency standard than the well-known 'clock transitions' between $m=0$ levels at zero magnetic field.

PACS numbers: 32.80.Pj, 42.62.Fi, 31.30.Gs, 32.60.+i

I. INTRODUCTION

In recent years, optical frequency standards based on single trapped ions and neutral atoms held in optical lattices have made remarkable progress [1, 2] towards achieving the elusive goal [3] of a fractional frequency stability of 10^{-18} . In $^{199}\text{Hg}^+$, $^{27}\text{Al}^+$, $^{171}\text{Yb}^+$, $^{115}\text{In}^+$, and $^{88}\text{Sr}^+$, optical frequencies of dipole-forbidden transitions have been measured [1, 4, 5, 6, 7]. Among the singly-charged alkali-earth ions, the odd isotope $^{43}\text{Ca}^+$ has been discussed as a possible optical frequency standard [8, 9] because of its nuclear spin $I = 7/2$ giving rise to transitions $4s^2S_{1/2}(F, m_F = 0) \leftrightarrow 3d^2D_{5/2}(F', m_{F'} = 0)$ that are independent of the first-order Zeeman effect. While the hyperfine splitting of the $S_{1/2}$ ground state has been precisely measured [10], the hyperfine splitting of the metastable $D_{5/2}$ has been determined with a precision of only a few MHz so far [11]. A precise knowledge of the $S_{1/2} \leftrightarrow D_{5/2}$ transition is also of importance for quantum information processing based on $^{43}\text{Ca}^+$ [12]. In these experiments where quantum information is encoded in hyperfine ground states, the quadrupole transition can be used for initialization of the quantum processor and for quantum state detection by electron shelving.

This paper describes the measurement of the hyperfine constants of the $D_{5/2}$ level by probing the quadrupole transition of a single trapped ion with a narrow-band laser. Our results confirm previous measurements and reduce the error bars on $A_{D_{5/2}}$ and $B_{D_{5/2}}$ by more than three orders of magnitude. In addition, we precisely measure the isotope shift of the transition with respect to $^{40}\text{Ca}^+$.

With a precise knowledge of the hyperfine structure constants at hand, the magnetic field dependence of

the $D_{5/2}$ Zeeman states is calculated by diagonalizing the Breit-Rabi Hamiltonian. It turns out that several transitions starting from one of the stretched states $S_{1/2}(F = 4, m_F = \pm 4)$ become independent of the first-order Zeeman shift at field values of a few Gauss. Transitions with vanishing differential Zeeman shifts at non-zero fields have been investigated in experiments with cold atomic gases [14] to achieve long coherence times and with trapped ions [15] for the purpose of quantum information processing. These transitions are also potentially interesting for building an optical frequency standard and have several advantages over $m_F = 0 \leftrightarrow m_{F'} = 0$ transitions. We experimentally confirm our calculations by mapping the field-dependence of one of these transitions.

II. EXPERIMENTAL SETUP

Our experiments are performed with a single $^{43}\text{Ca}^+$ ion confined in a linear Paul trap consisting of two tips and four blade-shaped electrodes [16]. A radio frequency voltage ($\nu_{rf} = 25.642$ MHz; $P_{rf} = 7$ W) is fed to a helical resonator and the up-converted signal is applied to one pair of blade electrodes while the other blade pair is held at ground. In such a way, a two-dimensional electric quadrupole field is generated which provides radial confinement for a charged particle if the radio frequency and amplitude are chosen properly. Two stainless steel tips are placed 5 mm apart in the trap's symmetry axis and are held at a positive voltage $U_{tips} = 1000$ V providing axial confinement. The electrodes are electrically isolated by Macor ceramics spacers which assure a $20\text{ }\mu\text{m}$ tolerance in the positioning of the four blades and the tip electrodes. For the parameters given above, the ion trap confines a $^{43}\text{Ca}^+$ ion in a harmonic potential with oscillation frequencies $\nu_{axial} = 1.2$ MHz and $\nu_{radial} = 4.2$ MHz in the axial and radial directions. Micromotion due to stray electric fields is compensated by applying voltages to two compensation electrodes. The correct compensation voltages are found by minimizing the Rabi frequency

*Electronic address: jan.benhelm@uibk.ac.at

†Present address: GE India Technology Center, Bangalore, India

‡URL: <http://www.quantumoptics.at>

of the first micromotional sideband of the quadrupole transition for two different laser beam directions. The trap is housed in a vacuum chamber with a pressure of about 10^{-10} mbar.

Single $^{43}\text{Ca}^+$ ions are loaded from an isotope-enriched source (Oak Ridge National Laboratory; 81.1 % $^{43}\text{Ca}^+$, 12.8 % $^{40}\text{Ca}^+$, 5.4 % $^{44}\text{Ca}^+$) into the trap by isotope-selective two-step photoionization [17, 18]. The first transition from the $4s\ ^1S_0$ ground state to the $4p\ ^1P_1$ excited state in neutral calcium is driven by an external cavity diode laser in Littrow configuration at 423 nm. Its frequency is monitored by saturation spectroscopy on a calcium vapor cell held at a temperature of 300 °C and by a wavelength meter with a relative accuracy of 10 MHz. The second excitation step connecting the $4p\ ^1P_1$ state to continuum states requires light with a wavelength below 390 nm. In our experiment, it is driven by a free-running laser diode at 375 nm.

For laser cooling, a grating-stabilized diode laser is frequency-doubled to produce light at 397 nm for exciting the $S_{1/2} \leftrightarrow P_{1/2}$ transition (see Fig. 1). By means of polarization optics and an electro-optical modulator operated at 3.2 GHz, laser beams exciting the following transitions are provided:

beam n°	polarization	transition
1, 2	π, σ^+	$S_{1/2}(F=4) \leftrightarrow P_{1/2}(F'=4)$
3	σ^+	$S_{1/2}(F=3) \leftrightarrow P_{1/2}(F'=4)$

Laser beams n° 1-3 are all switched on for Doppler cooling and fluorescence detection. We avoid coherent population trapping by lifting the degeneracy of the Zeeman sub-levels with a magnetic field. To avoid population trapping in the $D_{3/2}$ manifold, repumping laser light at 866 nm has to be applied. The repumping efficiency was improved by tuning the laser close to the $D_{3/2}(F=3) \leftrightarrow P_{1/2}(F'=3)$ transition frequency and red-shifting part of the light by $-f_1, -f_1 - f_2$ with two acousto-optical modulators (AOMs) operating at frequencies $f_1 = 150$ MHz and $f_2 = 245$ MHz. In this manner, all hyperfine $D_{3/2}$ levels are resonantly coupled to one of the $P_{1/2}(F' = 3, 4)$ levels. Since the electronic g-factor of the $D_{3/2}(F=3)$ level vanishes, coherent population trapping in this level needs to be avoided by either polarization-modulating the laser beam or by coupling the level to both $P_{1/2}(F' = 3, 4)$ levels. In our experiment, non-resonant light ($\delta \approx 190$ MHz) exciting the $D_{3/2}(F=3) \leftrightarrow P_{1/2}(F'=4)$ seems to be sufficient for preventing coherences from building up. After switching off laser beam n° 1, the ion is optically pumped into the state $S_{1/2}(F=4, m_F=4)$. The pumping efficiency is better than 95 %.

All diode lasers are stabilized to Fabry-Perot cavities. The cavity spacer is a block of Zerodur suspended in a temperature stabilized vacuum housing. For frequency tuning, one of the reference cavity mirrors is mounted using two concentric piezo transducers that are compensated for thermal drift. This allows frequency tuning the

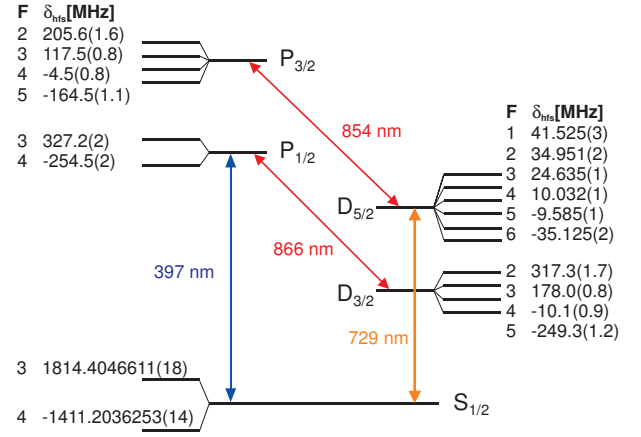


FIG. 1: $^{43}\text{Ca}^+$ level scheme showing the hyperfine splitting of the lowest energy levels. Hyperfine shifts δ_{hfs} of the levels are quoted in MHz (the splittings are taken from [10, 11] and our own measurement). Laser light at 397 nm is used for Doppler cooling and detection, the lasers at 866 nm and 854 nm pump out the D-states. An ultrastable laser at 729 nm is used for spectroscopy on the quadrupole transition.

lasers over several GHz while achieving low drift rates (typically < 100 Hz/s) once the piezos have settled.

To set the magnitude and orientation of the magnetic field, a single $^{40}\text{Ca}^+$ ion was loaded into the trap. The ambient magnetic B-field was nulled by applying currents to magnetic field compensation coils so as to minimize the ion's fluorescence. After that, the magnetic field can be set to the desired value by sending a current through a pair of coils defining the quantization axis. All coils are powered by homemade current drivers having a relative current instability of less than $2 \cdot 10^{-5}$ in 24 h.

Light for the spectroscopy on the $S_{1/2} \leftrightarrow D_{5/2}$ quadrupole transition is generated by a Ti:Sa laser stabilized to an ultra-stable high finesse reference cavity (finesse $\mathcal{F} = 410000$) [13]. The free spectral range of the cavity was measured to be $\Delta_{\text{FSR}} = 1933.07309(20)$ MHz by using a second independently stabilized laser and observing the beat note for the Ti:Sa laser locked to several different modes. From this measurement, also an upper limit of less than 50 Hz could be determined for the laser line width. The frequency drift of the 729 nm laser stabilized to the reference cavity is typically less than 0.5 Hz/s. By locking the laser to different modes of the reference cavity and by changing its frequency with AOMs we are able to tune the laser frequency in resonance with any transition between levels of $S_{1/2}$ and $D_{5/2}$ in $^{40}\text{Ca}^+$ and $^{43}\text{Ca}^+$. The radio frequencies applied to the AOMs are generated by a versatile frequency source based on direct digital synthesis.

Spectroscopy on the quadrupole transition is implemented using a pulsed scheme. In a first step, the ion is Doppler cooled and prepared in the $S_{1/2}(F=4, m_F = \pm 4)$ level by optical pumping. Then the ion is probed on the quadrupole transition by light at 729 nm. At the end of the experimental cycle, the ion's quantum state is de-

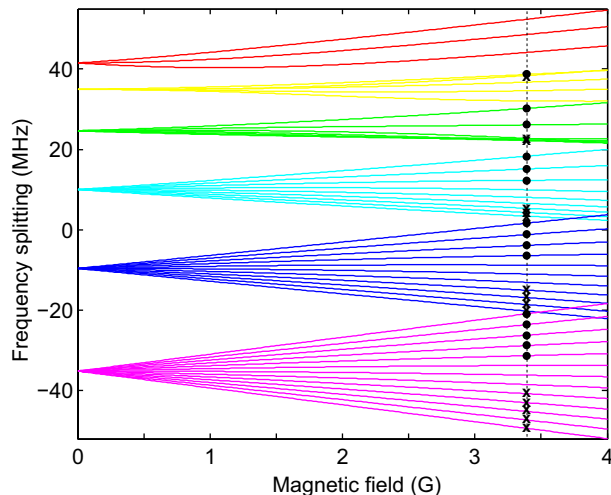


FIG. 2: Hyperfine and Zeeman splitting of the $D_{5/2}$ state manifold calculated for hyperfine constants measured in our experiment. Filled circles (●) and crosses (x) mark states that can be excited starting from the $S_{1/2}(F=4)$ state with magnetic quantum number $m_F = +4$ ($m_F = -4$), respectively. The vertical dashed line indicates the magnetic field used for measuring the frequency shifts in the experiment.

ected by a quantum jump technique. For this, the cooling laser and the repumper at 866 nm are turned back on for a duration of 5 ms, projecting the ion onto either the fluorescing $S_{1/2}$ or the dark $D_{5/2}$ state. The light emitted by the ion is collected with a customized lens system ($NA = 0.27$, transmission $> 95\%$) and observed on a photomultiplier tube and a CCD camera simultaneously. A threshold set for the number of photomultiplier counts discriminates between the two possibilities with high efficiency. Finally the $D_{5/2}$ state population is pumped back to $S_{1/2}$ by means of another grating-stabilized diode laser operating at 854 nm. This measurement cycle is repeated a hundred times before setting the probe laser to a different frequency and repeating the experiments all over again.

In order to set the magnetic field precisely, we use a single $^{40}\text{Ca}^+$ ion to determine the field strength by measuring the frequency splitting of the two transitions $S_{1/2}(m = +1/2) \leftrightarrow D_{5/2}(m' = +5/2)$ and $S_{1/2}(m = +1/2) \leftrightarrow D_{5/2}(m' = -3/2)$. Stray magnetic field oscillating at multiples of 50 Hz change the magnitude of the field by less than 2 mG over one period of the power line frequency. By synchronizing the experiments with the phase of the power line, ac-field fluctuations at multiples of 50 Hz are eliminated as a source of decoherence. As the duration of a single experiment typically is on the order of 20 ms, this procedure does not significantly slow down the repetition rate of the experiments.

III. RESULTS

A. Hyperfine coefficients for the $D_{5/2}$ state

The hyperfine structure splitting of the $S_{1/2}$ and $D_{5/2}$ states is determined by effective Hamiltonians [19] $H_{hfs}^{(S_{1/2})} = hA_{S_{1/2}}\mathbf{I} \cdot \mathbf{J}$ and, assuming that J is a good quantum number,

$$H_{hfs}^{(D_{5/2})} = hA_{D_{5/2}}\mathbf{I} \cdot \mathbf{J} + hB_{D_{5/2}} \frac{3(\mathbf{I} \cdot \mathbf{J})^2 + \frac{3}{2}(\mathbf{I} \cdot \mathbf{J}) - I(I+1)J(J+1)}{2I(2I-1)J(2J-1)} \quad (1)$$

operating on the hyperfine level manifolds of the ground and metastable state. Here, h is the Planck constant and $A_{D_{5/2}}$ ($A_{S_{1/2}}$) and $B_{D_{5/2}}$ are the hyperfine constants describing the magnetic dipole and electric quadrupole interactions in the $D_{5/2}$ ($S_{1/2}$) state; higher-order multipoles [20] are not taken into account. Terms arising from second-order perturbation theory [20] are expected to shift the levels by only negligible amounts as $(A_{D_{5/2}} \cdot A_{D_{3/2}})/\Delta_{FS} \approx 100$ Hz where Δ_{FS} denotes the fine-structure splitting of the D states.

In a non-zero magnetic field, the Hamiltonian (1) is replaced by

$$H^{(D_{5/2})} = H_{hfs}^{(D_{5/2})} + g_{D_{5/2}}\mu_B\mathbf{J} \cdot \mathbf{B} + g_I'\mu_B\mathbf{I} \cdot \mathbf{B}, \quad (2)$$

where $g_{D_{5/2}}$ is the electronic g-factor of the $D_{5/2}$ state and g_I' denotes the nuclear g-factor. Fig. 2 shows the resulting energy shifts of the Zeeman level caused by hyperfine and Zeeman interactions. The energies of the $S_{1/2}(F=4, m_F = \pm 4)$ levels used in our spectroscopic measurements are linearly shifted by $h\delta_{\pm} = \pm(g_{S_{1/2}}\frac{1}{2} + g_I'I)\mu_BB$.

From earlier measurements and calculations of the isotope shift [21] and the hyperfine splitting of the $S_{1/2}$ [10] and the $D_{5/2}$ [11, 22, 23] states, the transition frequencies on the quadrupole transition in $^{43}\text{Ca}^+$ are known to within 20 MHz with respect to the transition in $^{40}\text{Ca}^+$. This enabled us to unambiguously identify the lines observed in spectra of the $S_{1/2} \leftrightarrow D_{5/2}$ transition. In a first series of measurements the ion was prepared in the state $S_{1/2}(F=4, m_F = +4)$ by optical pumping with σ_+ -polarized light. There are fifteen transitions to the $D_{5/2}$ levels allowed by the selection rules for quadrupole transitions. Spectra were recorded on all of them with an excitation time of 500 μs in a magnetic field of about 3.40 G. In a second measurement series, after pumping the ion into $S_{1/2}(F=4, m_F = -4)$ another fifteen transitions were measured. To obtain the hyperfine constants of the $D_{5/2}$ state, we fitted the set of 30 transition frequencies by diagonalizing the Hamiltonian taking the hyperfine constants $A_{D_{5/2}}$, $B_{D_{5/2}}$, the magnetic field B and a frequency offset as free parameters. The hyperfine constant $A_{S_{1/2}} = -806.4020716$ MHz was measured in reference [10]. The g-factors $g_I' = 2.0503 \cdot 10^{-4}$ and

$g_{S_{1/2}} = 2.00225664$ were taken from references [24] and [25], $g_{D_{5/2}} = 1.2003(1)$ was measured by us in an experiment with a single $^{40}\text{Ca}^+$ ion. The fit yields

$$A_{D_{5/2}} = 3.8931(2) \text{ MHz},$$

$$B_{D_{5/2}} = 4.241(4) \text{ MHz},$$

where the standard uncertainty of the determination is added in parentheses. The average deviation between the measured and the fitted frequencies is about 1 kHz. If $g_{D_{5/2}}$ is used as a free parameter, we obtain $g_{D_{5/2}} = 1.2002(2)$ and the fitted values of the hyperfine constants do not change. Also, adding a magnetic octupole interaction [20] to the hyperfine Hamiltonian does not change the fit values of the hyperfine constants.

B. Isotope shift

After having determined the values of $A_{D_{5/2}}$ and $B_{D_{5/2}}$, the line center of the $^{43}\text{Ca}^+ S_{1/2} \leftrightarrow D_{5/2}$ transition can be found. By comparing the transition frequencies in $^{43}\text{Ca}^+$ and in $^{40}\text{Ca}^+$, the isotope shift $\Delta_{iso}^{43,40} = \nu_{43} - \nu_{40}$ is determined. Switching the laser from ν_{40} to ν_{43} is achieved by locking the laser to a TEM_{00} cavity mode three modes higher ($\nu_{n+3} = \nu_n + 3\Delta_{FSR}$) than for $^{40}\text{Ca}^+$ and adjusting its frequency with an AOM. For the isotope shift, we obtain

$$\Delta_{iso}^{43,40} = 4134.713(5) \text{ MHz}.$$

This value is in good agreement with a previous measurement ($\Delta_{iso}^{43,40} = 4129(18) \text{ MHz}$ [10]). Frequency drift between the measurements, accuracy of the reference cavity's free spectral range Δ_{FSR} and the uncertainty in the determination of the exact line centers limit the accuracy of our measurement.

C. Magnetic field independent transitions

Given the measured values of the hyperfine coefficients $A_{D_{5/2}}$, $B_{D_{5/2}}$, we calculate that there are seven transitions starting from the stretched states $S_{1/2}(F = 4, m_F = \pm 4)$ that have no first order Zeeman effect for suitably chosen magnetic fields in the range of 0-6 G. These transitions are useful as they offer the possibility of measuring the line width of the spectroscopy laser in the presence of magnetic field noise. To demonstrate this property, we chose the transition $S_{1/2}(F = 4, m_F = 4) \leftrightarrow D_{5/2}(F = 4, m_F = 3)$ which has the lowest second-order dependence on changes in the magnetic field. We measured the change in transition frequency for magnetic fields ranging from one to six Gauss as shown in figure 3. The black curve is a theoretical calculation based on the measurement of the hyperfine constants. For the data, the frequency offset is the only parameter that was adjusted to match the calculated curve. Both, the experi-

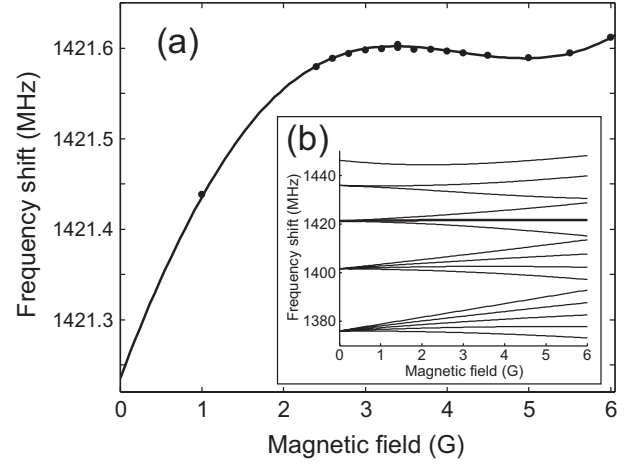


FIG. 3: (a) Frequency dependence of the $S_{1/2}(F = 4, m_F = 4) \leftrightarrow D_{5/2}(F = 4, m_F = 3)$ transition frequency for low magnetic fields. The transition frequency becomes field-independent at $B=3.38 \text{ G}$ and $B=4.96 \text{ G}$ with a second-order Zeeman shift of $\pm 16 \text{ kHz/G}^2$. The measured data are not corrected for the drift of the reference cavity which may lead to errors in the shift of about 1-2 kHz. To match the data with the theoretical curve based on the previously measured values of $A_{D_{5/2}}$, $B_{D_{5/2}}$, an overall frequency offset was adjusted. (b) Calculated shift of the fifteen allowed transitions starting from $S_{1/2}(F = 4, m_F = 4)$. The thick line shows the transition to the state $D_{5/2}(F' = 4, m_{F'} = 3)$.

mental data and the model show that the transition frequency changes by less than 400 kHz when the field is varied from 0 to 6 G. The transition frequency becomes field-independent at about $B=3.38 \text{ G}$ with a second order B-field dependency of -16 kHz/G^2 , which is six times less than the smallest coefficient for a clock transition based on $m_F = 0 \leftrightarrow m_{F'} = 0$ transitions at zero field. At $B=4.96 \text{ G}$ the linear Zeeman shift vanishes again.

We used the field-independence of this transition for investigating the phase coherence of our spectroscopy laser. For this, we set the magnetic field to 3.39 G and recorded an excitation spectrum of the transition by scanning the laser over the line with an interrogation time of 100 ms. The result is depicted in figure 4. A Gaussian fit gives a line width of 42 Hz. The observed line width is not yet limited by the life time τ of the $D_{5/2}$ state ($\tau = 1.17 \text{ s}$) or by the chosen interrogation time. Line broadening caused by magnetic field fluctuations can be excluded on this transition. Also, ac-Stark shifts are expected to play only a minor role. Therefore, we believe that the observed line width is mostly related to the line width of the exciting laser.

IV. SUMMARY AND DISCUSSION

The hyperfine structure of the $D_{5/2}$ level in $^{43}\text{Ca}^+$ has been observed and precisely measured by observing frequency intervals of the $S_{1/2}(F = 4, m_F = \pm 4) \leftrightarrow$

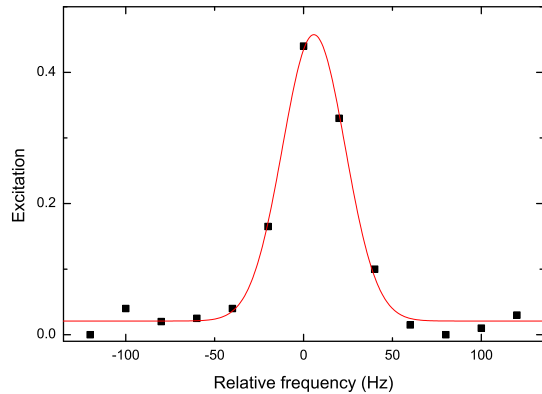


FIG. 4: Frequency scan over the transition $S_{1/2}(F=4, m_F=4) \leftrightarrow D_{5/2}(F'=4, m_{F'}=3)$ with an interrogation time of 100 ms. A Gaussian fit (solid line) determines a width of 42 Hz which is dominated by the line width of the spectroscopy laser at 729 nm.

$D_{5/2}(F' = 2 \dots 6, m_{F'})$ transitions at non-zero field. These measurements yielded values for the hyperfine constants $A_{D_{5/2}}$, $B_{D_{5/2}}$ as well as a determination of the isotope shift of the quadrupole transition with respect to $^{40}\text{Ca}^+$. A diagonalization of the $D_{5/2}$ state's Hamiltonian showed that several transitions exist which become magnetic-field independent at small but non-zero values of B . These transitions are of practical importance for probing the laser line width of the spectroscopy laser and

for monitoring the drift rate of its reference cavity. For the purpose of building an optical frequency standard based on $^{43}\text{Ca}^+$ [8, 9], they might be superior to the transitions $S_{1/2}(F, m_F=0) \leftrightarrow D_{5/2}(F', m_{F'}=0)$ for the following reasons: (i) the initialization step requires only optical pumping to the stretched state $S_{1/2}(F=4, m_F=\pm 4)$ which can be conveniently combined with resolved sideband cooling to the motional ground state of the external potential. (ii) The magnetic field can be exactly set to the value where the transition becomes field-independent while still maintaining a well-defined quantization axis. (iii) The second-order Zeeman effect can be reduced to a value that is six times smaller than what can be achieved for the best $m_F=0 \leftrightarrow m_{F'}=0$ 'clock transition'. Still, we are somewhat cautious about the usefulness of $^{43}\text{Ca}^+$ as an optical frequency standard as compared to other candidate ions. While the rather small hyperfine splitting of the metastable state has the nice property of providing field-independent transitions at low magnetic fields, it risks also to be troublesome as the induced level splitting is about the same size as typical trap drive frequencies. Improperly balanced oscillating currents in the trap electrodes might give rise to rather large ac-magnetic level shifts.

Acknowledgments

We wish to acknowledge support by the Institut für Quanteninformation GmbH and by the U. S. Army Research Office. We acknowledge P. Pham's contribution to the development of a versatile source of shaped RF pulses.

-
- [1] W. H. Oskay *et al.*, Phys. Rev. Lett. **97**, 020801 (2006).
 - [2] M. M. Boyd *et al.*, arXiv:physics/0611067.
 - [3] H. G. Dehmelt, IEEE Trans. Instr. Meas. **31**, 83 (1982).
 - [4] J. C. Bergquist, private communication.
 - [5] T. Schneider, E. Peik, and Chr. Tamm, Phys. Rev. Lett. **94**, 230801 (2005).
 - [6] J. v. Zanthier *et al.*, Opt. Lett. **25** 1729 (2000).
 - [7] H. S. Margolis *et al.*, Science **306**, 1355 (2004).
 - [8] C. Champenois *et al.*, Phys. Lett. A **331**, 298 (2004).
 - [9] M. Kajita, Y. Li, K. Matsubara, K. Hayasaka, and M. Hosokawa, Phys. Rev. A **72**, 043404 (2005).
 - [10] F. Arbes, M. Benzing, Th. Gudjons, F. Kurth, and G. Werth, Z. Phys. D **31**, 27 (1994).
 - [11] W. Nörtershäuser *et al.*, Eur. Phys. J. D **2**, 33 (1998).
 - [12] A. Steane, Appl. Phys. B **64**, 623 (1997).
 - [13] M. Notcutt, L.-S. Ma, J. Ye, and J. L. Hall, Opt. Lett. **30**, 1815 (2005).
 - [14] D. M. Harber, H. J. Lewandowski, J. M. McGuirk, and E. A. Cornell, Phys. Rev. A **66**, 053616 (2002).
 - [15] C. Langer *et al.*, Phys. Rev. Lett. **95**, 060502 (2005).
 - [16] F. Schmidt-Kaler *et al.*, Appl. Phys. B **77**, 789 (2003).
 - [17] D. Lucas *et al.*, Phys. Rev. A **69**, 012711 (2004).
 - [18] S. Gulde, D. Rotter, P. Barton, F. Schmidt-Kaler, R. Blatt, and W. Hogervorst, Appl. Phys. B **73**, 861 (2001).
 - [19] L. Armstrong, *Theory of the hyperfine structure of free atoms* (John Wiley & Sons, New York, 1971).
 - [20] C. Schwartz, Phys. Rev. **97**, 380 (1955).
 - [21] F. Kurth, T. Gudjons, B. Hilbert, T. Reisinger, G. Werth, and A.-M. Mårtensson-Pendrill, Z. Phys. D **34**, 227 (1995).
 - [22] B. K. Sahoo *et al.*, J. Phys. B **36**, 1899 (2003).
 - [23] K. Yu, L. Wu, B. Gou, and T. Shi, Phys. Rev. A **70**, 012506 (2004).
 - [24] N. J. Stone, At. Data Nucl. Data Tables **90**, 75 (2005).
 - [25] G. Tommaseo, T. Pfeil, G. Revalde, G. Werth, P. Indelicato, and J. P. Desclaux, Eur. Phys. J. D **25**, 113 (2003).